1 **Running title:** Study of post-transcriptional regulation in pigs

2

Modeling microRNA-driven post-transcriptional regulation

by using exon-intron split analysis (EISA) in pigs

5 Emilio Mármol-Sánchez[1*], Susanna Cirera[2], Laura M. Zingaretti[3], Mette Juul Jacobsen[2],

6 Yuliaxis Ramayo-Caldas[4], Claus B. Jørgensen[2], Merete Fredholm[2], Tainã Figueiredo

7 Cardoso[1†], Raquel Quintanilla[4], Marcel Amills[1,5]

8

9 [1]Centre for Research in Agricultural Genomics (CRAG), CSIC-IRTA-UAB-UB,

10 Universitat Autònoma de Barcelona, 08193 Bellaterra, Spain. [2]Department of

11 Veterinary and Animal Sciences, Faculty of Health and Medical Sciences, University of

12 Copenhagen, 1871 Frederiksberg C, Denmark. [3]Universidad Nacional de Villa María,

13 Villa María, Córdoba, Argentina. [4]Animal Breeding and Genetics Program, Institute for

14 Research and Technology in Food and Agriculture (IRTA), Torre Marimon, 08140

15 Caldes de Montbui, Barcelona, Spain. [5]Departament de Ciència Animal i dels Aliments,

16 Universitat Autònoma de Barcelona, 08193 Bellaterra, Barcelona, Spain.

17

18 *Emilio Mármol-Sánchez current affiliation: [1]Department of Molecular Biosciences,

19 The Wenner-Gren Institute, Stockholm University, Stockholm, Sweden. [2]Centre for

20 Paleogenetics, Stockholm University, Stockholm, Sweden.

21

22 [†]Tainã Figueiredo Cardoso current affiliation: Embrapa Pecuária Sudeste, Empresa

23 Brasileira de Pesquisa Agropecuária (EMBRAPA), 13560-970, São Carlos, SP, Brazil.

24

25   **Corresponding author:** Emilio Mármol-Sánchez. Science for Life Laboratory,

26   Department of Molecular Biosciences, The Wenner-Gren Institute. Stockholm

27   University, Stockholm, Sweden. Email: emilio.marmol.sanchez@gmail.com

28

29   Emilio Mármol-Sánchez: emilio.marmol.sanchez@gmail.com

30   Susanna Cirera: scs@sund.ku.dk

31   Laura M. Zingaretti: m.lau.zingaretti@gmail.com

32   Mette Juul Jacobsen: pmn418@alumni.ku.dk

33   Yuliaxis Ramayo-Caldas: yuliaxis@gmail.com; yuliaxis.ramayo@irta.cat

34   Claus B. Jørgensen: clausbj@sund.ku.dk

35   Merete Fredholm: mf@sund.ku.dk

36   Tainã Figueiredo Cardoso: tainafcardoso@gmail.com

37   Raquel Quintanilla: raquel.quintanilla@irta.cat

38   Marcel Amills: Marcel.Amills@uab.cat

39

40

41

42

43

44

45

46

47

48

2

Abstract

The contribution of microRNAs (miRNAs) to mRNA regulation has often been explored by *post hoc* selection of downregulated genes and determining whether they harbor binding sites for miRNAs of interest. This approach, however, does not discriminate whether these mRNAs are also downregulated at the transcriptional level. Here, we have characterized the transcriptional and post-transcriptional changes of mRNA expression in two porcine tissues: *gluteus medius* muscle of fasted and fed Duroc gilts and adipose tissue of lean and obese Duroc-Göttingen minipigs. Exon-intron split analysis (EISA) of RNA-seq data allowed us to identify downregulated mRNAs with high post-transcriptional signals in fed or obese states, and we assessed whether they harbor binding sites for upregulated miRNAs in any of these two physiological states. We found 26 downregulated mRNAs with high post-transcriptional signals in the muscle of fed gilts and 21 of these were predicted targets of upregulated miRNAs also in the fed state. For adipose tissue, 44 downregulated mRNAs in obese minipigs displayed high post-transcriptional signals, and 25 of these were predicted targets of miRNAs upregulated in the obese state. These results suggest that the contribution of miRNAs to mRNA repression is more prominent in the skeletal muscle system. Finally, we identified several genes that may play relevant roles in the energy homeostasis of the pig skeletal muscle (*DKK2* and *PDK4*) and adipose (*SESN3* and *ESRRG*) tissues. By differentiating transcriptional from post-transcriptional changes in mRNA expression, EISA provides a valuable view about the regulation of gene expression, complementary to canonical differential expression analyses.

Keywords: Exon-intron split analysis, microRNA, pigs, energy homeostasis.

3

Introduction

The post-transcriptional regulation of gene expression plays a fundamental role towards shaping fine-tuned biological responses to environmental changes (Schaefke *et al.* 2018). Such regulation can take place at multiple levels including splicing, 3′-cleavage and polyadenylation, decay or translation, and its main effectors are RNA binding proteins and non-coding RNAs (Schaefke *et al.* 2018). Of particular importance are microRNAs (miRNAs), which are primarily engaged in the post-transcriptional control of gene expression through inhibition of translation and/or degradation of target mRNAs (Bartel, 2018).

Multiple differential expression studies have been performed in pigs during the last decade (Pérez-Montarelo *et al.* 2013; Óvilo *et al.* 2014; Pilcher *et al.* 2015; Horodyska *et al.* 2018; Benítez *et al.* 2019). One of the main limitations of these studies is that the transcriptional and post-transcriptional components of gene regulation are not independently analyzed. This means that genes that are transcriptionally upregulated and post-transcriptionally downregulated, or vice versa, might not be detected as significantly differentially expressed. Another disadvantage of this approach is that it does not provide insights about the causes of the observed downregulation of RNA transcripts. For instance, studies have typically focused on specific sets of downregulated genes harboring binding sites for miRNAs, in order to disentangle regulatory functions driven by miRNAs (Han *et al.* 2017; Xie *et al.* 2019; Ali *et al.* 2021). This approach, however, cannot distinguish between transcriptional or post-transcriptional repression, which is essential to understand at which level of the mRNA life-cycle regulation is taking place.

To overcome this important limitation, Gaidatzis *et al.* (2015) devised the *exon-intron split analysis* (EISA), which separates the transcriptional and post-transcriptional

99   components of gene regulation by comparing the amounts of exonic and intronic reads

100   from expressed mRNA transcripts. The main assumption of this method is that intronic

101   reads are mainly derived from nascent unprocessed mRNAs or pre-mRNAs, so they

102   reflect transcriptional changes, while post-transcriptional changes can be inferred from

103   differences between the levels of the exonic and intronic fractions (Ameur *et al.* 2011;

104   Gaidatzis *et al.* 2015). For instance, a gene showing little to no differences in the

105   number of sequenced intronic reads, but a strong downregulation of exonic reads after a

106   certain treatment or challenge (nutrition, infection, temperature etc.), could be subjected

107   to post-transcriptional repression (Gaidatzis *et al.* 2015; Cursons *et al.* 2018; Pillman *et*

108   *al.* 2019). Recent developments on this principle have also been applied to infer the

109   transcriptional fate of cells (La Manno *et al.* 2018).

110   The main goal of the present study was to investigate the contribution of miRNAs to

111   post-transcriptional regulatory responses using the EISA methodology, combined with

112   *in silico* prediction of miRNA-mRNA interactions and covariation analyses in porcine

113   skeletal muscle and adipose tissues.

114

115

Materials and methods

Experimental design, sampling and processing

118   Two experimental systems were used:

119   (i) Duroc pigs: Twenty-three gilts were subjected to two fasting/feeding regimes, i.e. 11

120   gilts (*AL-T0*) were slaughtered in fasting condition, while 12 gilts (*AL-T2*) were

121   slaughtered after 7 h of having access to food (Cardoso *et al*. 2017; Ballester *et al*.

122   2018; Mármol-Sánchez *et al*. 2020). Immediately after slaughtering, *gluteus medius*

123   (GM) skeletal muscle samples were collected and snap-frozen at -80°C.

124 (ii) Duroc-Göttingen minipig F$_2$ inter-cross: Ten individuals fed *ad libitum* with

125 divergent fatness profiles for body mass index (BMI, 5 *lean* and 5 *obese*) were selected

126 from the UNIK resource population (Kogelman *et al.* 2013; Jacobsen *et al.* 2019).

127 Retroperitoneal adipose tissue was collected at slaughter and mature adipocytes were

128 subsequently isolated as previously reported (Jacobsen *et al.* 2019). UNIK minipigs

129 BMI profiles are detailed in **Table S1.**

130 RNA-seq and small RNA-seq expression data generated in the framework of these two

131 experimental systems have been described previously (Cardoso *et al.* 2017; Jacobsen *et*

132 *al.* 2019; Mármol-Sánchez *et al.* 2020). Sequencing reads from the RNA-seq and small

133 RNA-seq datasets were trimmed with the Cutadapt software (Martin, 2011). RNA-seq

134 reads were then mapped with the HISAT2 aligner (Kim *et al.* 2019) using default

135 parameters. The Bowtie Alignment v.1.2.1.1 software (Langmead *et al.* 2009) was used

136 to align small RNA-seq reads by considering small sequence reads specifications

137 (*bowtie -n 0 -m 20 -k 1 --best*). The Sscrofa11.1 porcine reference assembly (Warr *et al.*

138 2020) was used for mapping.

139

140 **Exon/Intron quantification**

141 We generated exonic and intronic-specific annotations spanning all available genes by

142 using the Sscrofa.11.1 v.103 gene annotation (Ensembl repositories:

143 http://ftp.ensembl.org/pub/release-103/gtf/sus_scrofa/). Overlapping intronic/exonic

144 regions (10 bp at both ends of introns), as well as singleton positions were removed

145 (Lawrence *et al.* 2013). We then used the *featureCounts* tool (Liao *et al.* 2014) to

146 independently quantify exon and intron expression levels for each mRNA encoding

147 gene, as well as expression levels of mature miRNAs.

148

Differential expression analyses

149

150 Canonical differential expression analyses were carried out with the *edgeR* tool

151 (Robinson *et al.* 2010) by considering only the exonic counts of mRNAs and the

152 miRNA expression levels measured in the two experimental systems under study. Only

153 genes showing average expression values above 1 count-per-million in at least 50% of

154 animals within each treatment group (*AL-T0* and *AL-T2* for GM tissue and *lean* and

155 *obese* for adipocyte isolates) were retained for further analyses. Expression filtered raw

156 counts for exonic mRNA and miRNA reads were normalized with the trimmed mean of

157 M-values normalization (TMM) method (Robinson & Oshlack 2010) and the statistical

158 significance of mean expression differences was tested with a quasi-likelihood F-test

159 (Robinson *et al.* 2010). Multiple hypothesis testing correction was implemented with

160 the false discovery rate method (Benjamini & Hochberg 1995). Messenger RNAs were

161 considered to be significantly differentially expressed when the absolute value of the

162 fold-change (FC) was higher than 2 ($|FC| > 2$) and the q-value < 0.05. Fasting Duroc

163 gilts (*AL-T0*) as well as UNIK *obese* minipigs were classified as baseline controls in

164 differential expression analyses, i.e. any given upregulation in exonic counts represents

165 and overexpression of the corresponding gene in fed (*AL-T2*) Duroc gilts or *lean* UNIK

166 minipigs with respect to their fasting (*AL-T0*) and *obese* counterparts, respectively.

167 Since changes in the expression of miRNAs are often subtler than those of mRNAs, the

168 thresholds to consider a miRNA as truly differentially expressed were set to $|FC| > 1.5$

169 and q-value < 0.05 (Guo *et al.* 2015) for fasted (*AL-T0*) vs fed (*AL-T2*) Duroc gilts.

170 Given the relatively low statistical significance of miRNA expression changes observed

171 in *obese* vs *lean* minipigs, we considered, as potential miRNA regulators, those that

172 were significantly (FC < -1.5; q-value < 0.05) and suggestively (FC > 1.5 and P-value $<$

173 0.01) upregulated in *lean* minipigs.

7

174

Exon/intron split analysis (EISA).

We applied EISA to differentiate transcriptional from post-transcriptional changes in mRNA expression in our two experimental systems (muscle and fat). Normalization was performed independently for exon and intron counts as described by Gaidatzis *et al.* (2015). Exonic and intronic gene abundances were subsequently $\log_2$ transformed, adding a pseudo-count of 1 and averaged within each considered treatment group. Only genes for which both exonic and intronic read counts were successfully quantified were further considered. Observed differences in each ith gene were expressed as the increment of exonic/intronic counts in fed (*AL-T2*) and *obese* animals with respect to fasting (*AL-T0*) and *lean* animals, respectively. In this way, the increment of intronic and exonic counts was calculated considering $\Delta Int = Int_{2i} - Int_{1i}$ and $\Delta Ex = Ex_{2i} - Ex_{1i}$, respectively. The magnitudes of the transcriptional (Tc) and post-transcriptional (PTc) changes in mRNA expression were then calculated. The Tc contribution to the observed counts is explained by ΔInt (Pillman *et al.* 2019), while PTc can be deduced from $\Delta Ex - \Delta Int$. In this way, the significance of Tc scores was assessed as in canonical differential expression analyses but using the intronic fraction as input. Besides, for assessing the statistical significance of PTc scores, we incorporated the fraction type (exonic or intronic counts) as an interaction term with the condition type (fasted *AL-T0* vs fed *AL-T2* or *obese* vs *lean*) in the framework of the generalized linear model (Gaidatzis *et al.* 2015) and using *edgeR* tool with a quasi-likelihood F-test as in differential expression analyses (Robinson *et al.* 2010). Both Tc and PTc components were z-scored to make ΔEx and ΔInt estimates comparable. Moreover, Tc and PTc scores were considered significant when $|FC| > 2$ and q-value < 0.05. Multiple hypothesis testing correction was implemented by using the false discovery rate approach (Benjamini & Hochberg 1995).

8

199   In order to obtain a prioritized list of genes showing high signals of post-transcriptional

200   regulation, the top 5% of expressed genes with the most negative PTc scores were

201   retrieved (irrespective of their statistical significance after multiple testing correction).

202   From these, we only focused on genes showing strongly reduced ΔEx values of at least

203   2-fold for post-transcriptional signals in both experimental systems (i.e. ΔEx < -1 in the

204    $\log_2$ scale). All implemented analyses have been summarized in **Fig. S1**. A ready-to-use

205   modular   pipeline   for   running   EISA   is   publicly   available   at

206   https://github.com/emarmolsanchez/EISAcompR.

207

208   **miRNA target prediction**

209   Putative interactions between the seed of expressed miRNAs (2nd-8th 5' nts) and the 3'-

210   UTRs of expressed mRNA genes were predicted on the basis of sequence identity using

211   the Sscrofa11.1 reference assembly and the seedVicious v1.1 tool (Marco 2018). The

212   annotated 3'-UTRs longer than 30 nts from porcine mRNAs were retrieved from

213   http://www.ensembl.org/biomart, while mature miRNA sequences were obtained from

214   miRBase (Kozomara *et al.* 2019). Redundant seeds from mature porcine microRNAs

215   were removed, and 8mer, 7mer-m8 and 7mer-A1 miRNA-mRNA interactions were

216   taken into account (Bartel 2018).

217   Based on Grimson *et al.* (2007), *in silico*-predicted miRNA-mRNA interactions

218   matching any of the following criteria were removed: (i) Binding sites located in 3'-

219   UTRs at less than 15 nts close to the end of the open reading frame (and the stop codon)

220   or less than 15 nts close to the terminal poly(A) tail (E criterion), (ii) binding sites

221   located in the middle of the 3'-UTR in a range comprising 45-55% of the central region

222   of the non-coding sequence (M criterion), and (iii) binding sites that lack AU-rich

223   sequences in their immediate upstream and downstream flanking regions comprising 30

9

224 nts each (AU criterion). A schematic representation of such criteria is available at **Fig.**

225 **S2**.

226 Covariation patterns between miRNAs and their predicted mRNA targets were assessed

227 by computing Spearman's correlation coefficients (ρ) with the TMM normalized and

228 log$_2$ transformed expression profiles of the exonic fraction of mRNA and miRNA

229 genes. Only miRNA-mRNA predicted pairs comprising significantly upregulated

230 miRNAs and downregulated mRNA genes with high PTc scores (see exon/intron split

231 analysis section) were considered.

232

233 **miRNA target enrichment analyses**

234 We predicted which downregulated mRNA genes, from those with highly negative

235 post-transcriptional signals, are putatively targeted by at least one significantly

236 upregulated miRNA. Subsequently, we investigated whether the sets of mRNA genes

237 identified in this way are more enriched in binding sites for upregulated miRNAs than

238 the whole set of expressed mRNAs genes with available 3'-UTRs (control background).

239 Enrichment analyses were carried out using the Fisher's exact test in R. Significance

240 level was set at a nominal P-value < 0.05.

241 We also tested whether downregulated mRNA genes with highly negative post-

242 transcriptional signals were significantly enriched to be targets of at least one of the top

243 5% most highly expressed miRNA genes (considering their overall average expression

244 and excluding significantly upregulated miRNAs), as well as of significantly

245 downregulated miRNAs.

246 As an additional control randomized test for enrichment analyses between miRNAs and

247 downregulated mRNAs with highly negative post-transcriptional signals, we

248 implemented a bootstrap corrected iteration to generate 100 random sets of 10 expressed

249   mature miRNA genes without seed redundancy. In this way, we predicted which

250   downregulated mRNA genes, from those with highly negative post-transcriptional

251   signals, are putatively targeted by at least one miRNA of the random sets generated. The

252   distribution of odds ratios obtained after enrichment tests over each random set of

253   miRNAs (N = 100) were then compared with the observed odds ratios obtained with the

254   set of significantly upregulated miRNAs.

255   The *P*-value for the significance of the deviation of observed odds ratios against the

256   bootstrapped odds ratios distribution was defined as:

257   $P - value = 1 - \frac{r+1}{k+1}$, where r is the number of permuted odds ratios with values

258   equal or higher than the observed odds ratio, and k is the number of permutations (N =

259   100).

260

261   **Gene covariation network and covariation enrichment score**

262   We used *edgeR* to identify differentially expressed genes in the *AL-T0* vs *AL-T2* (N =

263   454 genes) and *obese* vs *lean* (N = 299 genes) comparisons showing *q*-value < 0.05

264   after multiple testing correction. Then, the normalized exonic and intronic estimates in

265   the $\log_2$ scale obtained from EISA analyses were independently used to compute

266   Spearman's correlation coefficients (ρ). Significant correlations were identified with the

267   Partial Correlation with Information Theory (PCIT) algorithm (Reverter & Chan 2008)

268   implemented in the *pcit* R package (Watson-Haigh *et al.* 2010). In this way, the number

269   of overall significant pairwise correlations was compared with that obtained when only

270   considering the set of downregulated mRNA genes with highly negative post-

271   transcriptional signals and putatively targeted by significantly upregulated miRNAs.

272   Thus, the potential contribution of miRNAs to the observed differences in covariation

273   among the two sets of genes was assessed by calculating a covariation enrichment score

11

274   (CES), as reported by Tarbier *et al.* (2020). Further details about the algorithm used to

275   calculate the CES values and control tests can be found in **Supplementary Methods**.

276   Significant differences among the set of exonic, intronic and control CES values were

277   tested with a Mann-Whitney U non-parametric test (Mann & Whitney 1947).

278

279   **Verification of RNA-seq expression profiles by qPCR**

280   By using qPCR, we have verified that the expression profiles of selected mRNAs and

281   miRNAs highlighted in the adipose tissue experiment were in accordance with those

282   obtained with RNA-seq and small RNA-seq data. Since this experiment is just a control

283   of the quality of expression estimates, further details are reported in **Supplementary**

284   **Methods**. Primers for mRNA and miRNA qPCR expression profiling are available at

285   **Table S2**. Raw Cq values for each assay are available at **Table S3**.

286

287

288   # Results

289   **The analysis of post-transcriptional regulation in muscle samples from fasting and**

290   **fed Duroc gilts**

291   *Differential expression and EISA analyses*

292   Total RNA and small RNA were independently sequenced in muscle samples from

293   fasting (*AL-T0*) and fed (*AL-T2*) Duroc gilts. About 45.2 million reads (93%) per

294   sample from protein coding and non-coding genes were successfully mapped against the

295   Sscrofa.11.1 assembly when analyzing the GM muscle total RNA-seq data. Besides,

296   around 2.2 million reads per sample (42%) obtained from the small RNA-seq

297   experiment were successfully mapped to 370 annotated porcine miRNA genes.

298   A total of 30,322 (based on exonic reads) and 22,769 (based on intronic reads) genes

299   were successfully quantified after splitting the reference genome assembly between

300   exonic and intronic features. Exonic counts were ~23 fold more abundant than those

301   corresponding to intronic regions.

302   By using *edgeR*, we detected 454 mRNA genes with *q*-value < 0.05 (**Table S4a**).

303   Among these, only genes with |FC| > 2 were retained, resulting in 52 upregulated and 80

304   downregulated genes (**Table S4a** in bold and **Fig. S3a**). The analysis of small RNA-seq

305   data with *edgeR* revealed 16 miRNAs significantly differentially expressed, of which 8

306   were upregulated in *AL-T2* gilts. These 8 miRNAs, which represented 6 unique miRNA

307   seeds (ssc-miR-148a-3p, ssc-miR-7-5p, ssc-miR-30-3p, ssc-miR-151-3p, ssc-miR-374a-

308   3p and ssc-miR-421-5p; **Table S5** in bold), were selected as potential post-

309   transcriptional regulators of mRNA genes.

310   On the other hand, EISA highlighted 26 mRNA genes displaying the top 5% negative

311   PTc scores with at least 2-fold ΔEx reduction (**Table 1** and **Fig. S3b**). Eighteen out of

312   these 26 genes (69.23%) appeared as significantly downregulated (FC < -2; *q*-value <

313   0.05, **Table 1** and **Table S4b** in bold) according to differential expression analyses.

314   Also, we detected 133 mRNA genes with significant PTc scores (|FC| > 2; *q*-value <

315   0.05, **Table S6a**), of which three experienced at least a 2-fold reduction of their ΔEx

316   fraction (**Table S6a** in bold). Two out from these three mRNA genes ranked within

317   those with the top 5% negative PTc scores (**Table 1** and **Table S6a**). Among this set of

318   133 genes, only seven (5.26%) were also significantly differentially expressed (**Table**

319   **S6a**).

320   Moreover, with EISA we detected 344 genes displaying significant Tc scores (|FC| > 2;

321   *q*-value < 0.05, **Table S6b**) and among these, 71 (20.63%) were also significantly

322   differentially expressed (**Tables S6b**). Besides, 91 out of these 344 genes (26.45%) also

323   showed significant PTc scores (**Table S6b** in bold), but none of them were among the

324   mRNA genes displaying the top 5% negative PTc scores with at least 2-fold ΔEx

325   reduction (N = 26, **Table 1**). The whole list of expressed mRNA genes after differential

326   expression analyses is available at **Table S4c**. The whole lists of expressed mRNA

327   genes after EISA and their PTc and Tc scores are available at **Table S6c** and **S6d**,

328   respectively.

329

330   *Context-based pruning of predicted miRNA-mRNA interactions removes spurious*

331   *unreliable target events*

332   Before making *in silico* predictions of miRNA-mRNA interactions, we investigated

333   their reliability (**Table S7**). To do so, we first evaluated the enrichment in the number of

334   genes with binding sites for at least one of the 6 non-redundant miRNAs upregulated in

335   the GM muscle of *AL-T2* gilts (ssc-miR-148a-3p, ssc-miR-7-5p, ssc-miR-30-3p, ssc-

336   miR-151-3p, ssc-miR-374a-3p and ssc-miR-421-5p) over a random background of

337   expressed genes with no context-based removal of predicted binding sites (see

338   Methods). Introducing additional context-based filtering criteria to remove unreliable

339   binding site predictions resulted in an overall increased enrichment of target genes

340   within the list of the top 1% (N = 13 genes, **Fig. S4a**) and 5% (N = 26 genes, **Fig. S4b**)

341   genes with negative PTc scores and displaying at least 2-fold ΔEx reduction. This

342   significant enrichment was more evident when using the AU criterion, as shown in **Fig.**

343   **S4a**.

344

345

346

14

Table 1: mRNA genes with the top 5% post-transcriptional (PTc) scores and at least 2-fold exonic fraction (ΔEx) reduction (equivalent to -1 in the $\log_2$ scale) of *gluteus medius* skeletal muscle samples from fasting (*AL-T0*, N = 11) and fed (*AL-T2*, N = 12) Duroc gilts.

ID	Gene	$\log_2 FC^a$	ΔEx^b	PTc^c	*P*-value	*q*-value	DE^d	miRNA target
ENSSSCG00000032094	*DKK2*	-2.010	-1.431	-4.738	1.654E-05	3.830E-03		x
ENSSSCG00000015334	*PDK4*	-2.108	-5.250	-4.698	4.693E-03	1.330E-01	x	x
ENSSSCG00000015037	*IL18*	-1.655	-1.191	-3.682	4.787E-03	1.340E-01	x	x
ENSSSCG00000005385	*NR4A3*	-1.337	-3.082	-3.646	4.038E-02	4.098E-01	x	
ENSSSCG00000003766	*DNAJB4*	-1.391	-1.008	-3.348	8.358E-03	1.905E-01		x
ENSSSCG00000015969	*CHRNA1*	-1.561	-1.339	-3.341	2.606E-03	9.406E-02	x	x
ENSSSCG00000039419	*SLCO4A1*	-1.055	-2.279	-3.180	2.820E-02	3.544E-01	x	x
ENSSSCG00000049158		-1.107	-1.096	-3.164	3.182E-02	3.735E-01		
ENSSSCG00000004347	*FBXL4*	-1.298	-1.126	-3.133	1.422E-03	6.520E-02	x	x
ENSSSCG00000004979	*MYO9A*	-1.239	-1.003	-3.043	7.296E-03	1.731E-01		x
ENSSSCG00000013351	*NAV2*	-1.163	-1.196	-2.863	2.605E-04	2.301E-02	x	x
ENSSSCG00000032741	*TBC1D9*	-0.913	-1.061	-2.736	1.534E-02	2.583E-01		x
ENSSSCG00000031728	*ABRA*	-1.238	-1.393	-2.704	1.295E-03	6.116E-02	x	x
ENSSSCG00000006331	*PBX1*	-0.891	-1.039	-2.480	1.135E-02	2.177E-01		x
ENSSSCG00000035037	*SIK1*	-1.357	-1.289	-2.475	3.999E-03	1.212E-01	x	x
ENSSSCG00000038374	*CIART*	-1.027	-1.321	-2.052	1.543E-02	2.587E-01	x	
ENSSSCG00000023806	*LRRN1*	-0.776	-1.013	-1.983	1.580E-01	7.074E-01		x
ENSSSCG00000009157	*TET2*	-0.381	-1.123	-1.792	4.880E-01	9.582E-01		x
ENSSSCG00000011133	*PFKFB3*	-0.022	-2.256	-1.785	9.712E-01	9.987E-01	x	x
ENSSSCG00000002283	*FUT8*	-0.578	-1.286	-1.784	9.887E-02	6.059E-01	x	x
ENSSSCG00000023133	*OSBPL6*	-0.432	-1.088	-1.772	3.835E-01	9.108E-01	x	
ENSSSCG00000017986	*NDEL1*	-0.767	-1.644	-1.759	1.006E-02	2.081E-01	x	x
ENSSSCG00000031321	*NR4A1*	-0.630	-1.328	-1.720	6.298E-02	5.006E-01	x	
ENSSSCG00000035101	*KLF5*	-0.519	-1.487	-1.708	2.942E-01	8.488E-01	x	x
ENSSSCG00000004332	*BACH2*	-0.714	-2.105	-1.705	9.089E-02	5.861E-01	x	x
ENSSSCG00000017983	*PER1*	-0.773	-1.073	-1.627	3.000E-02	3.662E-01	x	

ENSSSCG00000049158 did not have any annotated 3´-UTR so it was excluded from further analyses. ^{a}Log$_2$FC: estimated $\log_2$ fold change for mean exonic fraction from *gluteus medius* skeletal muscle samples of fasted *AL-T0* and fed *AL-T2* Duroc gilts; ^{b}ΔEx: exonic fraction increment (Ex$_2$ – Ex$_1$) in $\log_2$ scale when comparing exon abundances in *AL-T0* (Ex$_1$) vs *AL-T2* (Ex$_2$) Duroc gilts; ^{c}PTc: post-transcriptional signal (ΔEx – ΔInt) in z-score scale. The *q*-value has been calculated with the false discovery rate approach (Benjamini & Hochberg 1995). ^{d}DE: Significantly differentially expressed (FC < -2; *q*-value < 0.05). The "x" symbols indicate significantly downregulated genes according to their exonic counts, as well as those mRNA genes targeted by at least one of the significantly upregulated miRNAs excluding redundant seeds (N = 6, **Table S5**).

15

360   *Several genes with relevant post-transcriptional signals detected with EISA are*

361   *predicted to be targets of upregulated miRNAs*

362   Target prediction and context-based pruning of miRNA-mRNA interactions for mRNA

363   genes displaying the top 5% negative PTc scores and at least 2-fold reduction in the

364   ΔEx exonic fraction (N = 26, **Table 1**, **Fig. 1a**) made possible to detect 11 8mer, 21

365   7mer-m8 and 22 7mer-A1 miRNA binding sites for the six non-redundant seeds of

366   miRNAs significantly upregulated in *AL-T2* gilts (**Table S5** in bold) in 21 out of the 26

367   analyzed mRNAs (80.77%, **Table S7**). Moreover, 14 out of these 21 genes (66.67%)

368   were also significantly differentially expressed (**Table 1** and **Table S4b** in bold).

369   This set of 21 mRNA genes with putative post-transcriptional repression mediated by

370   miRNAs showed a significant enrichment in 8mer, 7mer-m8 and 7mer-A1 sites for the

371   6 miRNAs significantly upregulated in *AL-T2* gilts, especially when combining these

372   three types of binding sites altogether (**Fig. 1b**). The miRNAs with the highest number

373   of significant miRNA-mRNA interactions were ssc-miR-30a-3p and ssc-miR-421-5p,

374   which showed nine and eight significant interactions, followed by ssc-miR-148-3p with

375   four significant interactions (**Table S7**).

376   We also evaluated the enrichment of the mRNA genes within the list of the top 5%

377   negative PTc scores and at least 2-fold ΔEx reduction (N = 26, **Table 1**) to be targets of

378   at least one of the following: (i) miRNAs downregulated in *AL-T2* fed gilts (**Table S5**),

379   (ii) top 5% most expressed miRNAs, excluding those significantly upregulated (ssc-

380   miR-1, ssc-miR-133a-3p, ssc-miR-26a, ssc-miR-10b, ssc-miR-378, ssc-miR-99a-5p,

381   ssc-miR-27b-3p, ssc-miR-30d, ssc-miR-486 and ssc-let-7f-5p), and (iii) random sets (N

382   = 100) of 10 expressed miRNAs, as a control test. In none of these three analyses a

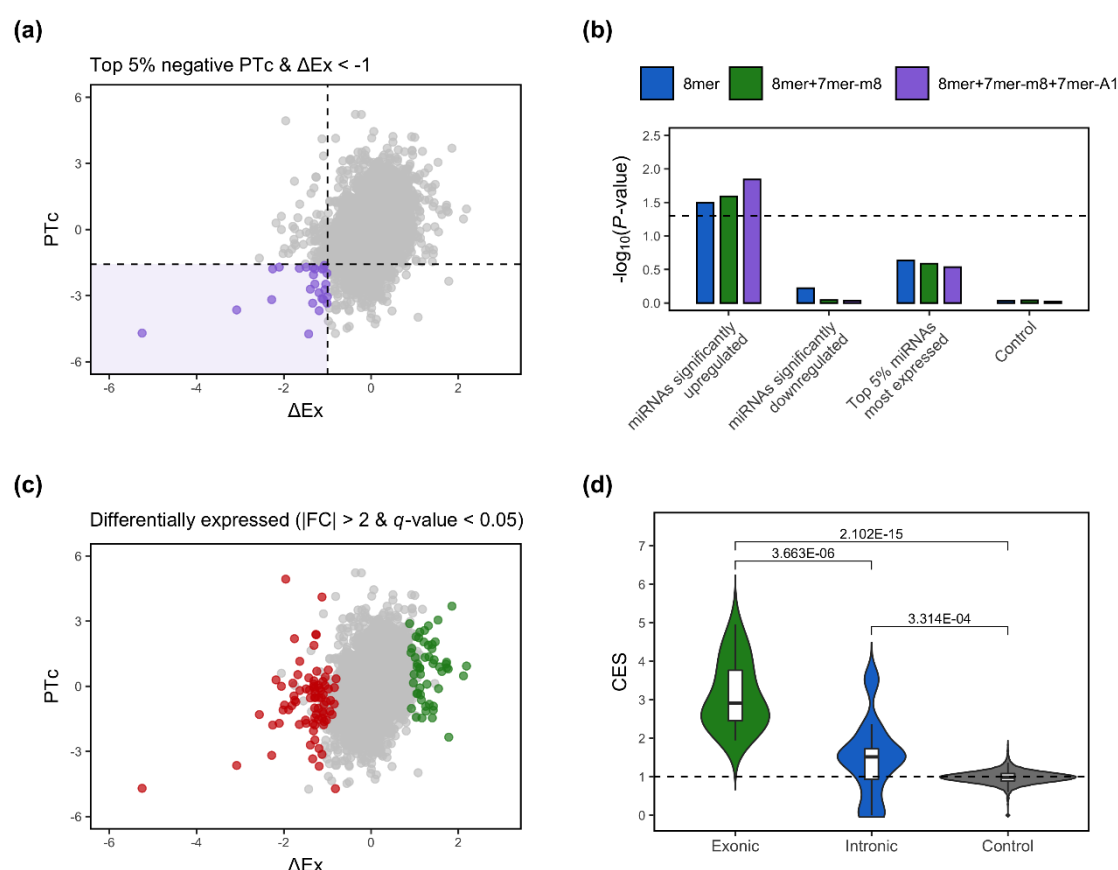383   significant enrichment was detected (**Fig. 1b**).

384   The mRNA with the highest negative and most significant PTc score was the Dickkopf

385   WNT Signaling Pathway Inhibitor 2 (*DKK2*), being a strong candidate to be repressed

386   by miRNAs (**Table 1**). Indeed, *DKK2* was the only gene harboring two miRNA 8mer

387   binding sites (**Table S7**). Interestingly, this locus was almost significantly differentially

388   expressed (**Table 1** and **Table S4b**). The discordance between EISA and differential

389   expression results can be fully appreciated when comparing **Fig. 1a** (genes with high

390   post-transcriptional repression after EISA) and **Fig. 1c** (differential expression

391   analyses), where only 18 out of the 26 mRNA genes detected with EISA appeared as

392   significantly downregulated in the *edgeR*-based differential expression analyses (**Table**

393   **1**). Although several of the mRNA genes shown in **Table 1** were highly downregulated

394   (**Table S4b**), the majority were mildly to slightly downregulated or not significantly

395   differentially expressed.

396

397   *Genes showing post-transcriptional regulatory signals predominantly covary at the*

398   *exonic level*

399   To further elucidate whether the set of 21 mRNA genes with putative post-

400   transcriptional repression mediated by upregulated miRNAs showed covarying

401   expression profiles, we evaluated the number of significant co-expressed pairs among

402   them and among the whole set of mRNA genes with *q*-value < 0.05, including those

403   from the set of 21 mRNA genes with *q*-value > 0.05 after differential expression

404   analyses (**Table 4b**).

405   By calculating CES values for both exonic and intronic fractions (see Methods) of the

406   21 genes putatively targeted by the 6 significantly upregulated miRNAs, our analyses

407   revealed that 19 out of these 21 genes showed increased covariation in their exonic

408   fraction when compared to their intronic fraction (**Table S8**, **Fig. 1d**), and *DKK2* was

409   again the gene with the strongest exonic covariation fold change compared to its

410   intronic covariation (**Table S8**). As expected, control random sets of genes (N = 1,000)

411   displayed CES ≈ 1, indicative of no covariation (**Fig. 1d**). The observed CES

412   distributions of exonic and intronic sets were significantly different (*P*-value = 3.663E-

413   06) after running non-parametric tests (**Fig. 1d**), thus supporting that the majority of

414   these 21 genes might be indeed co-regulated at the post-transcriptional level by

415   upregulated miRNAs.

416

417

418   **Figure 1:** (**a**) Scatterplot depicting genes expressed in *gluteus medius* skeletal muscle of

419   fasted (*AL-T0*, N = 11) and fed (*AL-T2*, N = 12) Duroc gilts according to their exonic

420   fraction (ΔEx) and post-transcriptional (PTc) scores. Genes with the top 5% negative

421   PTc scores and at least 2-fold ΔEx reduction (equivalent to -1 in the $\log_2$ scale) are

422   highlighted in purple and delimited by dashed lines. (**b**) Enrichment analyses comparing

18

423 all expressed mRNA genes and the set of mRNA genes with the top 5% negative PTc

424 scores and at least 2-fold ΔEx reduction as being putatively targeted by either

425 significantly upregulated miRNAs (FC > 1.5; *q*-value < 0.05), significantly

426 downregulated miRNAs (FC < -1.5; *q*-value < 0.05) or the top 5% most highly

427 expressed miRNAs, excluding significantly upregulated miRNAs. As indicated with the

428 dashed line, a nominal *P*-value = 0.05 was set as a significance threshold. (**c**) Scatterplot

429 depicting genes expressed in *gluteus medius* skeletal muscle of fasted (*AL-T0*, N = 11)

430 and fed (*AL-T2*, N = 12) Duroc gilts according to their exonic fraction (ΔEx) and post-

431 transcriptional (PTc) scores. Genes significantly upregulated are in green, while those

432 being downregulated are in red (|FC| > 2; *q*-value < 0.05). (**d**) Covariation enrichment

433 scores (CES) for the exonic and intronic fractions of the 21 mRNA genes with the top

434 5% negative PTc scores and at least 2-fold ΔEx reduction predicted to harbor binding

435 sites for upregulated miRNAs (N = 6) in the *gluteus medius* skeletal muscle of fasted

436 (*AL-T0*, N = 11) and fed (*AL-T2*, N = 12) Duroc gilts. The control set was established

437 by generating 1,000 permuted lists of 21 genes chosen at random and using their exonic

438 and intronic fractions for calculating their CES values. Statistical significance was

439 assessed using a Mann-Whitney U non-parametric test (Mann & Whitney 1947). The

440 dashed line represents a CES of 1, equivalent to an observed null fold change in

441 covariation.

442

443 **Studying post-transcriptional signals in adipose tissue using the UNIK minipig**

444 **population**

445 After pre-processing and filtering of sequenced reads from adipocyte samples, we were

446 able to retrieve ~98.1 and ~0.87 million mRNA and small RNA reads per sample, and

447 ~96.5% and ~73.4% of these reads mapped to annotated porcine mRNA and miRNA

448   genes, respectively. Differential expression analyses revealed a total of 299 genes with

449   *q*-value < 0.05, of which 52 and 95 were significantly downregulated and upregulated

450   (FC > |2|; *q*-value < 0.05), respectively (**Table S9a** in bold). Only one miRNA (ssc-

451   miR-92b-3p) was significantly upregulated in *lean* minipigs (**Table S10**), while six

452   additional miRNAs showed suggestive differential expression (*P*-value < 0.01), of

453   which four were upregulated (ssc-miR-148a-3p, ssc-miR-204, ssc-miR-92a and ssc-

454   miR-214-3p; **Table S10** in bold).

455   After running EISA, only the sestrin 3 (*SESN3*) gene showed a significant PTc score,

456   having the second highest negative PTc score (**Table 2** and **Table S11a**). Moreover,

457   *SESN3* was also detected as the most significantly downregulated gene by *edgeR* (**Table**

458   **S9a**). A total of 44 downregulated mRNAs in *lean* minipigs displayed the top 5% PTc

459   scores with reduced ΔEx of at least 2-fold (**Table 2** and **Fig. 2a**). Among them, only 12

460   (27.27%) appeared as significantly downregulated (FC < -2; *q*-value < 0.05, **Table 2**

461   and **Table S9b** in bold). The whole list of expressed genes after differential expression

462   analyses are available at **Table S9c**.

463   Twenty-five out of the 44 (58.14%, **Table S9b**) mRNAs downregulated in *lean*

464   minipigs and displaying the top 5% negative PTc scores were classified as putative

465   targets of the set of miRNAs upregulated in *lean* minipigs (N = 4, ssc-miR-92b-3p, ssc-

466   miR-148a-3p, ssc-miR-204 and ssc-miR-214-3p; **Table S10** in bold). Target prediction

467   and context-based pruning of miRNA-mRNA interactions for these 25 genes made

468   possible to detect eight 8mer, 21 7mer-m8 and 24 7mer-A1 miRNA binding sites

469   (**Table S12**) for upregulated miRNAs (N = 4) in *lean* UNIK minipigs (**Table S10**).

470   Again, the *SESN3* gene showed the highest number of predicted putative miRNA target

471   sites in its 3´-UTR (**Table S12**).

472　　Enrichment analyses for these 25 mRNAs (**Table 2**) revealed no significant enrichment

473　　for 8mer, 7mer-m8 and 7mer-A1 miRNA binding sites (**Fig. 2b**). Besides, only seven of

474　　them (26.92%) appeared as significantly downregulated (FC < -2; *q*-value < 0.05) in the

475　　differential expression analyses with *edgeR* (**Table S9b** and **Table 2**, **Fig. 2c**). The

476　　exonic fractions of 18 out of these 25 mRNA genes showed significantly increased

477　　covariation (*P*-value = 2.703E-02) compared to the covariation observed for the intronic

478　　fractions (**Fig. 2d** and **Table S13**).

479　　Regarding Tc scores, a total of 195 genes showed significant transcriptional signals

480　　(|FC| > 2; *q*-value < 0.05, **Table S11b**), and 48 of them were also significantly

481　　differentially expressed (24.61%, **Tables S9a** and **S11b**). Moreover, three of them

482　　(*ARHGAP27*, *CDH1* and *LEP*) were found among those with the top 5% post-

483　　transcriptional signals (**Table 2** and **Table S11b** in bold). The whole lists of expressed

484　　genes after EISA and their PTc and Tc scores are available at **Table S11c** and **S11d**,

485　　respectively.

486　　Results obtained for qPCR verification analyses are described in **Fig. S5**.

487

488　　**Table 2:** mRNA genes with the top 5% post-transcriptional (PTc) scores and at least 2-

489　　fold exonic fraction (ΔEx) reduction (equivalent to -1 in the log2 scale) of adipocytes

490　　from *lean* (N = 5) and *obese* (N = 5) UNIK minipigs classified in accordance with their

491　　body mass index.

mRNA	Gene	log$_2$FC[a]	ΔEx[b]	PTc[c]	*P*-value	*q*-value	DE[d]	miRNA target
ENSSSCG00000010814	*ESRRG*	-0.591	-5.305	-6.425	7.364E-01	9.996E-01		x
ENSSSCG00000037015	*SESN3*	-2.000	-1.378	-5.707	2.541E-07	2.477E-03	x	x
ENSSSCG00000032452	*WFS1*	-2.198	-2.138	-5.510	9.509E-03	9.996E-01	x	
ENSSSCG00000039548	*PTGFR*	-1.634	-1.590	-4.915	8.804E-03	9.996E-01		x
ENSSSCG00000013829	*SYDE1*	-1.670	-1.160	-4.188	5.795E-04	6.000E-01	x	
ENSSSCG00000002265	*FAM174B*	-1.244	-1.726	-4.179	5.385E-02	9.996E-01		x
ENSSSCG00000016233	*SERPINE2*	-1.735	-2.060	-3.603	5.684E-02	9.996E-01	x	x
ENSSSCG00000006243	*PENK*	-0.420	-2.104	-3.573	7.628E-01	9.996E-01		
ENSSSCG00000038879	*RELB*	-1.272	-1.056	-3.512	3.659E-03	9.996E-01	x	

21

Ensembl ID	Gene	Log2FC	ΔEx	PTc	q-value		x	x
ENSSSCG00000023408	SAMD4A	-1.328	-1.156	-3.509	4.486E-02	9.996E-01		x
ENSSSCG00000008449	SLC3A1	-1.014	-1.154	-3.491	5.859E-02	9.996E-01		
ENSSSCG00000014921	PRSS23	-1.141	-1.739	-3.360	2.719E-01	9.996E-01		x
ENSSSCG00000017186	RNF157	-1.218	-2.338	-3.317	2.413E-01	9.996E-01	x	x
ENSSSCG00000035403	RFX2	-1.109	-1.022	-2.958	1.550E-01	9.996E-01		x
ENSSSCG00000010893		-0.655	-1.352	-2.931	4.068E-01	9.996E-01		x
ENSSSCG00000031819	TP53I11	-1.002	-1.711	-2.883	4.102E-01	9.996E-01		x
ENSSSCG00000017137	METRNL	-0.674	-1.102	-2.812	2.422E-01	9.996E-01		
ENSSSCG00000032562	TMC6	-0.837	-1.152	-2.765	2.078E-01	9.996E-01		
ENSSSCG00000031261	RHOQ	-0.903	-1.046	-2.750	1.839E-02	9.996E-01		
ENSSSCG00000001089	GPLD1	-0.872	-1.761	-2.723	4.302E-01	9.996E-01		x
ENSSSCG00000034259	PMEPA1	-0.880	-1.348	-2.720	3.583E-01	9.996E-01		x
ENSSSCG00000017014	PANK3	-0.614	-1.037	-2.557	2.288E-01	9.996E-01		x
ENSSSCG00000003377	ACOT7	-0.790	-2.688	-2.544	3.439E-01	9.996E-01	x	
ENSSSCG00000010079	PPM1F	-0.762	-1.035	-2.473	4.967E-02	9.996E-01	x	x
ENSSSCG00000040464	LEP	-0.747	-2.186	-2.463	1.880E-01	9.996E-01	x	x
ENSSSCG00000022029	RAP1GAP	-0.120	-1.109	-2.418	8.822E-01	9.996E-01		x
ENSSSCG00000022099	TP53INP2	-0.628	-1.058	-2.403	3.683E-01	9.996E-01		
ENSSSCG00000025652	CDH1	-0.472	-2.592	-2.372	6.533E-01	9.996E-01		x
ENSSSCG00000027266	PNPLA3	-0.443	-1.386	-2.198	5.725E-01	9.996E-01		
ENSSSCG00000015401	PCLO	-0.674	-1.492	-2.182	4.537E-01	9.996E-01		x
ENSSSCG00000020872		-1.029	-1.128	-2.090	1.340E-01	9.996E-01		
ENSSSCG00000032633	FAM53A	-0.749	-1.033	-2.066	4.576E-02	9.996E-01	x	
ENSSSCG00000015559	NCF2	-0.679	-1.221	-2.061	3.570E-01	9.996E-01		x
ENSSSCG00000015766	WDR17	-0.609	-1.139	-1.998	2.093E-01	9.996E-01		
ENSSSCG00000009761	NCOR2	-0.681	-1.421	-1.913	2.643E-01	9.996E-01		
ENSSSCG00000016928	RAB3D	-0.491	-1.142	-1.888	2.953E-01	9.996E-01		
ENSSSCG00000011230	OSBPL10	-0.576	-1.594	-1.869	4.272E-01	9.996E-01		x
ENSSSCG00000017298	TANC2	-0.615	-1.541	-1.846	4.896E-01	9.996E-01		
ENSSSCG00000007899		-0.524	-1.036	-1.814	4.500E-01	9.996E-01		x
ENSSSCG00000026421	PKD2L2	-0.463	-1.230	-1.800	5.098E-01	9.996E-01		
ENSSSCG00000015332	PON1	-0.626	-1.076	-1.763	2.530E-01	9.996E-01	x	x
ENSSSCG00000009215	ABCG2	-0.455	-1.446	-1.749	5.684E-01	9.996E-01		
ENSSSCG00000017328	ARHGAP27	-0.235	-2.788	-1.699	8.113E-01	9.996E-01	x	x
ENSSSCG00000017199	TRIM47	-0.362	-1.057	-1.645	6.717E-01	9.996E-01		x

492

493 ENSSSCG00000016928 did not have an annotated 3´-UTR and was therefore excluded from further analyses.

494 [a]Log2FC: estimated $\log_2$ fold change for mean exonic fraction from adipocytes of *lean* and *obese* UNIK minipigs;

495 [b]ΔEx: exonic fraction increment ($Ex_2 - Ex_1$) in $\log_2$ scale when comparing exon abundances in obese (Ex_1) vs lean
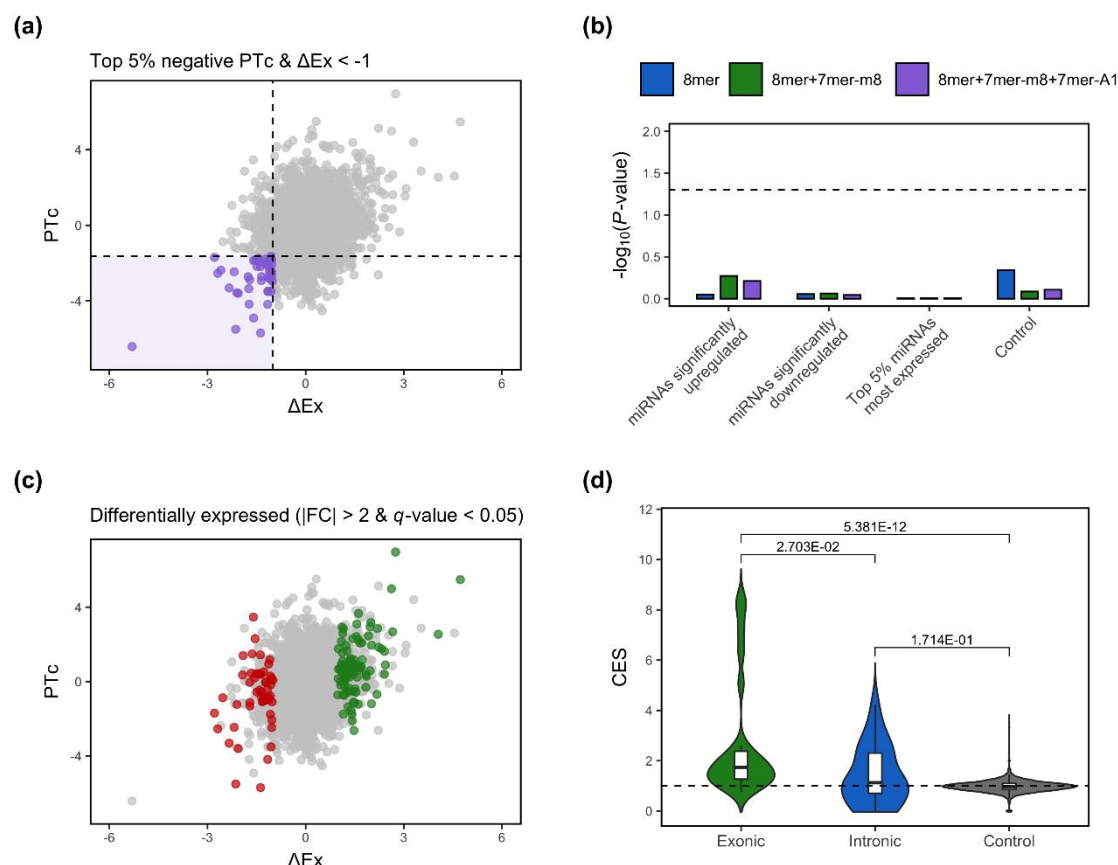
496 (Ex_2) UNIK minipigs; [c]PTc: post-transcriptional signal ($\Delta Ex - \Delta Int$) in z-score scale. The *q*-value has been calculated

497 with the false discovery rate (FDR) approach (Benjamini & Hochberg 1995); [d]DE: Significantly differentially

498 expressed (FC < -2; *q*-value < 0.05). The "x" symbols indicate significantly downregulated genes according to their

499 exonic counts, as well as those mRNA genes targeted by at least one of the significantly upregulated miRNAs

500 excluding redundant seeds (N = 4, **Table S10**).

501

Figure 2: (**a**) Scatterplot depicting genes expressed in adipocytes obtained from UNIK minipigs with *lean* (N = 5) and *obese* (N = 5) phenotypes (using their body mass index as reference) according to their exonic fraction (ΔEx) and post-transcriptional (PTc) scores. Genes with the top 5% negative PTc scores and at least 2-fold ΔEx reduction (equivalent to -1 in the $\log_2$ scale) are highlighted in purple and delimited by dashed lines. (**b**) Enrichment analyses comparing all expressed mRNA genes and the set of mRNA genes with the top 5% negative PTc scores and at least 2-fold ΔEx reduction as being putatively targeted by either significantly upregulated miRNAs (FC > 1.5; *q*-value < 0.05), significantly downregulated miRNAs (FC < -1.5; *q*-value < 0.05) or the top 5% most highly expressed miRNAs, excluding significantly upregulated miRNAs. As indicated with the dashed line, a nominal *P*-value = 0.05 was set as a significance threshold. (**c**) Scatterplot depicting genes expressed in adipocytes obtained from UNIK minipigs with *lean* (N = 5) and *obese* (N = 5) phenotypes (using their body mass index

23

515 as reference) according to their exonic fraction (ΔEx) and post-transcriptional (PTc)

516 scores. Genes significantly upregulated are in green, while those being downregulated

517 are in red (|FC| > 2; *q*-value < 0.05). (**d**) Covariation enrichment scores (CES) for the

518 exonic and intronic fractions of the 25 mRNA genes with the top 5% negative PTc

519 scores and at least 2-fold ΔEx reduction predicted to harbor binding sites for

520 upregulated miRNAs (N = 4) in adipocytes obtained from UNIK minipigs with *lean* (N

521 = 5) and *obese* (N = 5) phenotypes. The control set was established by generating 1,000

522 permuted lists of 25 genes chosen at random and using their exonic and intronic

523 fractions for calculating their CES values. Statistical significance was assessed using a

524 Mann-Whitney U non-parametric test (Mann & Whitney 1947). The dashed line

525 represents a CES of 1, equivalent to an observed null fold change in covariation.

526

527

Discussion

529 **Contribution of the Tc and PTc components of gene regulation to energy**

530 **homeostasis in porcine muscle and adipose tissues**

531 After running EISA on both muscle and adipose tissue datasets, we observed that the

532 number of genes with significant transcriptional signals (Tc) was much higher than that

533 of loci with significant post-transcriptional signals (PTc). Such difference evidences that

534 gene expression changes induced by feeding or obesity might be mostly driven by

535 transcriptional rather than post-transcriptional modulators. It is worth noting, however,

536 that few mRNAs showed post-transcriptional signals alone and were thus mixed with

537 transcriptional signals either in concordant or in opposite directions.

538 For prioritizing putative post-transcriptionally repressed mRNA genes by miRNAs, we

539 focused on those with the strongest observed downregulation based on their ΔEx values

24

540   (at least 2-fold reduction) and PTc signal (top 5% negative scores). Hence, we did not

541   consider the significance of PTc scores as a relevant criterion, as these will appear as

542   significant only when the post-transcriptional response is strong and not confounded by

543   a cooperative repressive transcriptional signal. Alternative thresholds other than the top

544   5% negative PTc scores or 2-fold for ΔEx fraction could be applied, depending on the

545   strength of the post-transcriptional signal detected.

546   Besides, it is worth noting that our RNA-seq data was generated following

547   manufacturer's instructions for TruSeq stranded libraries. This commonly used protocol

548   selects for poly(A) mRNAs, and the majority of non-poly(A) intronic lariats generated

549   after splicing will be lost, thus producing an artificial decrease in the quantified intronic

550   fraction (intronic reads). Although the intronic yield is decreased in poly(A) RNA

551   compared to total RNA protocols (Ameur *et al.* 2011), the recoverable intronic fraction

552   is still highly correlated with nascent transcription (Gaidatzis *et al.* 2015; La Manno *et*

553   *al.* 2018), probably derived from the presence of poly(A) introns or unspliced mRNAs

554   being sequenced, albeit at low abundance. Thus, the remaining intronic reads might

555   conform a limited and indirect yet representative proxy of the transcriptional activity.

556   Alternative methods for measuring such transcriptional activity by directly monitoring

557   transcription across the genome have also been applied (Patel *et al.* 2020), and might be

558   preferred over the use of intronic fractions. However, the implementation of such

559   alternatives is limited so far, and the relatively simple and cost-effective usage of

560   intronic reads present in already available RNA-seq data justifies the use of the EISA

561   approach.

562

563   **Differential expression analyses and EISA highlight different sets of genes**

25

564   Few genes with significant Tc and PTc components were also classified by *edgeR* as

565   significantly differentially expressed. Such a discrepancy between EISA and differential

566   expression analyses is in agreement with the subtle regulation elicited by miRNAs,

567   which is dependent on the expression level of miRNAs and the number of target sites

568   within a given mRNA 3'-UTR (Bartel 2018). In this way, EISA might serve as a good

569   approach to identify both strong and subtle post-transcriptional effects mediated by

570   miRNAs that canonical differential expression approaches might not be able to capture.

571   Importantly, these discrepancies were reduced when we focused on genes with top 5%

572   negative PTc scores and at least 2-fold reduction in their ΔEx values: as much as

573   69.23% (skeletal muscle) and 27.27% (adipose tissue) of such genes were also detected

574   as differentially expressed. This increase in concordance was more pronounced in the

575   skeletal muscle (fasted vs fed gilts) experimental system. This might be due to the

576   overall stronger upregulation of miRNAs observed for this dataset when compared with

577   that generated in the adipose tissue experiment, which can be explained by intrinsic

578   genomic differences among pig breeds, the tissues analyzed and/or the metabolic

579   challenge undertaken.

580

581   **Predicting the contribution of miRNAs to the post-transcriptional regulatory**

582   **response in porcine muscle and adipose tissues**

583   Since the efficacy of miRNA-based repression of mRNA expression depends on the

584   context of the miRNA binding site within the 3'-UTR (Grimson *et al.* 2007), we have

585   assessed the usefulness of introducing context-based filtering criteria for removing

586   spurious *in silico*-predicted binding sites for miRNAs. Using enrichment analyses, we

587   were able to link the expression of the set of mRNAs with downregulated exonic

588   fraction to the expression of upregulated miRNAs predicted to target them.

589   In the skeletal muscle system, prediction of miRNA binding sites in mRNA genes

590   displaying the top 5% negative post-transcriptional signals and at least 2-fold reduction

591   in their exonic fraction revealed that the majority of them (80.77%) harbored at least

592   one binding site for the corresponding set of significantly upregulated miRNAs (N = 6).

593   In contrast, such pattern was much less evident in the adipose tissue, which could be

594   explained by the fact that the majority of upregulated miRNAs in *lean* minipigs did not

595   reach significance.

596   Although we verified by qPCR the RNA-seq expression levels of selected

597   downregulated mRNAs and upregulated miRNAs in the UNIK adipose tissue

598   experiment, further experimental validation of the reported mRNA-miRNA interactions

599   is needed. *In silico* predictions of miRNA binding sites, EISA and covariation analyses

600   might be helpful to identify miRNA-mRNA pairs to be experimentally validated with

601   co-transfection gene reporter assays, in order to increase the yet scarce collection of

602   validated mRNA-miRNA interactions in domestic species.

603

604   **Covariation patterns in the expression of downregulated mRNAs predicted to be**

605   **targeted by upregulated microRNAs**

606   We further hypothesized that mRNA genes showing relevant post-transcriptional

607   downregulation might be repressed by the same set of significantly upregulated

608   miRNAs, which could induce shared covariation in the expression profiles of such

609   mRNAs at the exonic level. In contrast, their intronic fraction would be mainly

610   unaffected as introns would have been excised prior to any given miRNA-driven

611   downregulation. In this way, an increased gene covariation in downregulated mRNAs

612   with high post-transcriptional signals might be detectable at the exon but not at the

613   intron level. Indeed, our results revealed an increased covariation in downregulated

614   mRNAs with high post-transcriptional signals at their exonic fraction compared with

615   covariation patterns of their intronic fraction, suggesting that their expression might be

616   repressed by a common set of upregulated miRNAs.

617

618   **Genes displaying the strongest post-transcriptional signals in porcine skeletal**

619   **muscle and adipose tissue are involved in glucose and lipid metabolism**

620   The mRNA genes showing the strongest post-transcriptional downregulation in fasted

621   vs fed gilts displayed a variety of relevant biological functions. The *DKK2* gene showed

622   the most negative significant PTc score. This gene also displayed the strongest

623   covariation difference in its exonic fraction compared with the intronic one. This

624   consistent post-transcriptional regulatory effect might be mediated by ssc-miR-421-5p

625   and ssc-miR-30a-3p, two highly significantly upregulated miRNAs. The DKK2 protein

626   is a member of the dickkopf family, which inhibits the Wnt signaling pathway through

627   its interaction with the LDL-receptor related protein 6 (LRP6). Its repression has been

628   associated with reduced blood-glucose levels and improved glucose uptake (Li *et al.*

629   2012), as well as with improved adipogenesis (Yang & Shi 2021) and the inhibition of

630   aerobic glycolysis (Deng *et al.* 2019). These results are consistent with the increased

631   glucose usage and triggered adipogenesis in muscle tissue after nutrient supply. Other

632   relevant post-transcriptionally downregulated mRNAs detected with EISA were:

633   pyruvate dehydrogenase kinase 4 (*PDK4*), interleukin 18 (*IL18*), nuclear receptor

634   subfamily 4 group A member 3 (*NR4A3*), acetylcholine receptor subunit α (*CHRNA1*),

635   PBX homeobox 1 (*PBX1*), Tet methylcytosine dioxygenase 2 (*TET2*), BTB domain and

636   CNC homolog (*BACH2*), all of which are involved in the regulation of energy

637   homeostasis (Lindegaard *et al.* 2013; Zhang *et al.* 2014; Tamahara *et al.* 2017; Wu *et al.*

638   2018; Xu *et al.* 2019) and lipid metabolism in muscle cells (Monteiro *et al.* 2011;

639   Pearen *et al.* 2013) in response to nutrient uptake.

640   On the other hand, several genes with high post-transcriptional signals were not

641   predicted to be targets of upregulated miRNAs: the circadian associated repressor of

642   transcription (*CIART*) and period 1 (*PER1*), oxysterol binding protein like 6 (*OSBPL6*)

643   and nuclear receptor subfamily 4 group A member 1 (*NR4A1*). Interestingly, all of them

644   were significantly downregulated (Cardoso *et al.* 2017; Mármol-Sánchez *et al.* 2020).

645   An explanation to this might be that although miRNAs are key post-transcriptional

646   regulators, other alternative post-transcriptional effectors, such as long non-coding

647   RNAs (lncRNAs), circular RNAs (circRNAs) or RNA binding proteins (RBPs) might

648   be at play. Besides, indirect repression via upregulated miRNAs acting over regulators

649   of these genes, such as transcription factors, could be also a major influence on their

650   observed repression (Patel *et al.* 2020).

651   The use of EISA on expression data from adipocytes isolated from *obese* vs *lean* UNIK

652   minipigs revealed several mRNA genes with high post-transcriptional repression, which

653   are also involved in the regulation of lipid metabolism and energy homeostasis. The

654   gene showing the highest post-transcriptional signal was the estrogen related receptor γ

655   (*ESRRG*), which modulates oxidative metabolism and mitochondrial function in adipose

656   tissue and inhibits adipocyte differentiation when repressed (Kubo *et al.* 2009). Another

657   relevant locus identified with EISA was *SESN3*, an activator of the mTORC2 and

658   PI3K/AKT signaling pathway that promotes lipolysis when inhibited (Tao *et al.* 2015).

659   This gene showed the most significant downregulation in *lean* minipigs, and gathered

660   multiple putative binding sites for all the four upregulated miRNAs under study.

661   Other genes showing significant post-transcriptional downregulation were: sterile α

662   motif domain containing 4A (*SAMD4A*), prostaglandin F2- receptor protein (PTGFR),

29

663   serine protease 23 (PRSS23), ring finger protein 157 (*RNF157*), oxysterol binding

664   protein like 10 (*OSBPL10*), glycosylphosphatidylinositol phospholipase 1 (GPLD1),

665   RAP1 GTPase activating protein (RAP1GAP) and leptin (*LEP*), and all of which are

666   tightly linked to adipocyte differentiation (Perttilä *et al.* 2009; Martínez *et al.* 2013;

667   Chen *et al.* 2014; Kosacka *et al.* 2018) or energy homeostasis (Ussar *et al.* 2012; Wang

668   *et al.* 2018; Izquierdo *et al.* 2019; Kuo *et al.* 2020). Despite the overall weak influence

669   of putative miRNA-driven downregulation on mRNAs expressed in adipocytes, we

670   were able to identify a set of genes with high post-transcriptional signals indicative of

671   putative miRNA-derived repression and tightly related to adipose tissue metabolism

672   regulation. However, non-miRNA transcriptional and post-transcriptional modulators,

673   might also contribute to such repression.

674

675

Conclusions

677   EISA applied to study gene regulation in porcine skeletal muscle and adipose tissues

678   showed that more genes were subjected to transcriptional rather than post-

679   transcriptional regulation, suggesting that changes in mRNA levels are mostly driven by

680   factors acting at the transcriptional level. More importantly, the concordance between

681   the sets of significantly differentially expressed genes and those with significant Tc or

682   PTc scores was quite limited, but improved (mostly in the skeletal muscle experiment)

683   when we prioritized the downregulated genes with the top 5% negative post-

684   transcriptional signals. Nevertheless, many of the genes with relevant PTc signals were

685   not among the top significantly downregulated loci, thus demonstrating the usefulness

686   of complementing differential expression analyses with the EISA approach. In the

687   skeletal muscle, we detected several mRNAs predicted to be co-regulated by a common

688   set of miRNAs. In contrast, in the adipose tissue such relationship was more subtle,

689   suggesting that the contribution of miRNAs to mRNA repression might be affected by

690   tissue type, breed and/or intrinsic experimental factors. Finally, EISA made possible to

691   identify several genes related with carbohydrate and lipid metabolism, which may play

692   relevant roles in the energy homeostasis of the skeletal muscle and adipose tissues. By

693   differentiating the transcriptional from the post-transcriptional changes in mRNA

694   expression, EISA provides a valuable view, complementary to differential expression

695   analysis, about the miRNA-driven regulation of gene expression.

696

697

698   **Ethics approval**

699   Animal care and management procedures for Duroc gilts followed national guidelines

700   for the Good Experimental Practices and were approved by the Ethical Committee of

701   the Institut de Recerca i Tecnologia Agroalimentàries (IRTA). Animal care and

702   management procedures for UNIK minipigs were carried out according to the Danish

703   "Animal Maintenance Act" (Act 432 dated 9 June 2004).

704

705   **Availability of data**

706   The RNA-seq and small RNA-seq datasets from skeletal muscle tissue used in the

707   current study are available at the Sequence Read Archive (SRA) database with

708   BioProject codes PRJNA386796 and PRJNA595998, respectively. For the adipose

709   tissue samples, RNA-seq and small RNA-seq datasets are available at PRJNA563583

710   and PRJNA759240.

711

712   **Competing interests**

713   The authors declare that they have no competing interests

714

722

723   **Authors' contributions**

724   The authors' responsibilities were as follows: M.A. and R.Q. generated the total RNA

725   and small RNA sequencing data corresponding to the GM muscle, respectively. S.C.,

726   M.J.J., C.B.J. and M.F produced the total RNA sequencing corresponding to the adipose

727   tissue. M.A., R.Q., S.C., M.J.J., C.B.J., M.F., T.F.C. and E.M.-S. conducted the

728   research. S.C. performed qPCR analyses. E.M.-S. analyzed the data. L.M.Z. contributed

729   to bioinformatic analyses. Y.R.-C. contributed to critical assessment. M.A. and

730   R.Q. secured funding for the study. E.M.-S., S.C. and M.A. drafted the manuscript. All

731   authors contributed to manuscript corrections, read and approved the final manuscript.

732

742

743

References

745   Ali A., Murani E., Hadlich F., Liu X., Wimmers K. & Ponsuksili S. (2021) In utero fetal

746   weight in pigs is regulated by microRNAs and their target genes. *Genes* **12**, 1264.

747   Ameur A., Zaghlool A., Halvardson J., Wetterbom A., Gyllensten U., Cavelier L. *et al.*

748   (2011) Total RNA sequencing reveals nascent transcription and widespread co-

749   transcriptional splicing in the human brain. *Nature Structural & Molecular*

750   *Biology* **18**, 1435–40.

751   Ballester M., Amills M., González-Rodríguez O., Cardoso T.F., Pascual M., González-

752   Prendes R. *et al.* (2018) Role of AMPK signaling pathway during compensatory

753   growth in pigs. *BMC Genomics* **9**, 682.

754   Bartel D.P. (2018) Metazoan microRNAs. *Cell* **173**, 20–51.

755   Benítez R., Trakooljul N., Núñez Y., Isabel B., Murani E., De Mercado E. *et al.* (2019)

756   Breed, diet, and interaction effects on adipose tissue transcriptome in Iberian and

757   duroc pigs fed different energy sources, *Genes* **10**, 589.

758   Benjamini Y. & Hochberg Y. (1995) Controlling the false discovery rate: a practical

759   and powerful approach to multiple testing. *Journal of the Royal Statistical*

760   *Society Series B (Methodological)* **57**, 289–300.

761   Cardoso T.F., Quintanilla R., Tibau J., Gil M., Mármol-Sánchez E., González-

762   Rodríguez O. *et al.* (2017) Nutrient supply affects the mRNA expression profile

33

763   of the porcine skeletal muscle. *BMC Genomics* **18**, 603.

764   Chen Z., Holland W., Shelton J.M., Ali A., Zhan X., Won S, *et al.* (2014) Mutation of

765   mouse *Samd4* causes leanness, myopathy, uncoupled mitochondrial respiration,

766   and dysregulated mTORC1 signaling. *Proceedings of the National Academy of*

767   *Sciences (USA)* **111**, 7367–7372.

768   Cursons J., Pillman K.A., Scheer K.G., Gregory P.A., Foroutan M., Hediyeh-Zadeh S.

769   *et al.* (2018) Combinatorial targeting by microRNAs co-ordinates post-

770   transcriptional control of EMT. *Cell Systems* **7**, 77-91.e7.

771   Deng F., Zhou R., Lin C., Yang S., Wang H., Li W. *et al.* (2019) Tumor-secreted

772   dickkopf2 accelerates aerobic glycolysis and promotes angiogenesis in colorectal

773   cancer. *Theranostics* **9**, 1001-1014.

774   Friedman R.C., Farh K.K.H., Burge C.B. & Bartel D.P. (2009) Most mammalian

775   mRNAs are conserved targets of microRNAs. *Genome Research* **19**, 92–105.

776   Gaidatzis D., Burger L., Florescu M. & Stadler M.B. (2015) Analysis of intronic and

777   exonic reads in RNA-seq data characterizes transcriptional and post-

778   transcriptional regulation. *Nature Biotechnology* **33**, 722–729.

779   Grimson A., Farh K.K.H., Johnston W.K., Garrett-Engele P., Lim L.P. & Bartel D.P.

780   (2007) MicroRNA targeting specificity in mammals: determinants beyond seed

781   pairing. *Molecular Cell* **27**, 91–105.

782   Guo Y., Liu J., Elfenbein S.J., Ma Y., Zhong M., Qiu C., Ding Y. *et al.* (2015)

783   Characterization of the mammalian miRNA turnover landscape. *Nucleic Acids*

784   *Research* **43**, 2326–2341.

785   Han H., Gu S., Chu W., Sun W., Wei W., Dang X. *et al.* (2017) miR-17-5p regulates

786   differential expression of NCOA3 in pig intramuscular and subcutaneous adipose

787   tissue. *Lipids* **52**, 939–949.

788   Horodyska J., Wimmers K., Reyer H., Trakooljul N., Mullen A.M., Lawlor P.G. *et al.*

789   (2018) RNA-seq of muscle from pigs divergent in feed efficiency and product

790   quality identifies differences in immune response, growth, and macronutrient and

791   connective tissue metabolism. *BMC Genomics* **19**, 791.

792   Izquierdo A.G., Crujeiras A.B., Casanueva F.F. & Carreira M.C. (2019) Leptin, obesity,

793   and leptin resistance: where are we 25 years later? *Nutrients* **11**, 2704.

794   Jacobsen M.J., Havgaard J.H., Anthon C., Mentzel C.M.J., Cirera S., Krogh P.M. *et al.*

795   (2019) Epigenetic and transcriptomic characterization of pure adipocyte fractions

796   from obese pigs identifies candidate pathways controlling metabolism. *Frontiers*

797   *in Genetics* **10**, 1268.

798   Kim D., Paggi J.M., Park C., Bennett C. & Salzberg S.L. (2019) Graph-based genome

799   alignment and genotyping with HISAT2 and HISAT-genotype. *Nature*

800   *Biotechnology* **37**, 907–915.

801   Kogelman L.J.A., Kadarmideen H.N., Mark T., Karlskov-Mortensen P., Bruun C.S.,

802   Cirera S. *et al.* (2013) An F2 pig resource population as a model for genetic

803   studies of obesity and obesity-related diseases in humans: Design and genetic

804   parameters. *Frontiers in Genetics* **4**, 29.

805   Kosacka J., Nowicki M., Paeschke S., Baum P., Blüher M. & Klö ting N. (2018) Up-

806   regulated autophagy: as a protective factor in adipose tissue of WOKW rats with

807   metabolic syndrome. Diabetology & Metabolic Syndrome **10**, 13.

808   Kozomara A., Birgaoanu M. & Griffiths-Jones S. (2019) MiRBase: From microRNA

809   sequences to function. *Nucleic Acids Research* **47**, D155–D162.

810   Kubo M., Ijichi N., Ikeda K., Horie-Inoue K., Takeda S. & Inoue S. (2009) Modulation

811   of adipogenesis-related gene expression by estrogen-related receptor γ during

812   adipocytic differentiation. *Biochimica et Biophysica Acta (BBA) Gene Regulatory*

813   *Mechanisms* **1789**, 71–77.

814   Kuo C.-S., Chen J.-S., Lin L.-Y., Schmid-Schönbein G.W., Chien S., Huang P.-H. *et al.*

815   (2020) Inhibition of serine protease activity protects against high fat diet-induced

816   inflammation and insulin resistance. *Scientific Reports* **10**, 1–11.

817   La Manno G., Soldatov R., Zeisel A., Braun E., Hochgerner H., Petukhov V. *et al.*

818   (2018) RNA velocity of single cells. *Nature* **560**, 494–498.

819   Langmead B., Trapnell C., Pop M. & Salzberg S.L. (2009) Ultrafast and memory-

820   efficient alignment of short DNA sequences to the human genome. *Genome*

821   *Biology* **10**, R25.

822   Lawrence M., Huber W., Pagès H., Aboyoun P., Carlson M., Gentleman R. *et al.* (2013)

823   Software for computing and annotating genomic ranges. *PLoS Computational*

824   *Biology* **9**, e1003118.

825   Li X., Shan J., Chang W., Kim I., Bao J., Lee H.-J. *et al.* (2012) Chemical and genetic

826   evidence for the involvement of Wnt antagonist Dickkopf2 in regulation of

827   glucose metabolism. *Proceedings of the National Academy of Sciences (USA)*

828   **109**, 11402–11407.

829   Liao Y., Smyth G.K. & Shi W. (2014) featureCounts: an efficient general purpose

830   program for assigning sequence reads to genomic features. *Bioinformatics* **30**,

831   923–930.

832   Lindegaard B., Mathews V.B., Brandt C., Hojman P., Allen T.L., Estevez E. *et al.*

833   (2013) Interleukin-18 activates skeletal muscle AMPK and reduces weight gain

834   and insulin resistance in mice. *Diabetes* **62**, 3064–3074.

835   Mann H.B. & Whitney D.R. (1947) On a test of whether one of two random variables is

836   stochastically larger than the other. *Annals of Mathematical Statistics* **18**, 50–60.

837   Marco A. (2018) SeedVicious: Analysis of microRNA target and near-target sites. *PLoS*

838   *One* 13, e0195532.

839   Mármol-Sánchez E., Ramayo-Caldas Y., Quintanilla R., Cardoso T.F., González-

840   Prendes R., Tibau J. *et al.* (2020) Co-expression network analysis predicts a key

841   role of microRNAs in the adaptation of the porcine skeletal muscle to nutrient

842   supply. *Journal of Animal Science & Biotechnology* **11**, 10.

843   Martin M. (2011) Cutadapt removes adapter sequences from high-throughput

844   sequencing reads. *EMBnet.Journal* **17**, 10.

845   Martínez P., Gómez-López G., García F., Mercken E., Mitchell S., Flores J.M. *et al.*

846   (2013) RAP1 protects from obesity through its extratelomeric role regulating

847   gene expression. *Cell Reports* **3**, 2059–2074.

848   Monteiro M.C., Sanyal M., Cleary M.L., Sengenès C., Bouloumié A., Dani C. *et al.*

849   (2011) PBX1: a novel stage-specific regulator of adipocyte development. *Stem*

850   *Cells* **29**, 1837–1848.

851   Óvilo C., Benítez R., Fernández A., Núñez Y., Ayuso M., Fernández A.I. *et al.* (2014)

852   Longissimus dorsi transcriptome analysis of purebred and crossbred Iberian pigs

853   differing in muscle characteristics. *BMC Genomics* **15**, 413.

854   Patel R.K., West J.D., Jiang Y., Fogarty E.A. & Grimson A. (2020) Robust partitioning

855   of microRNA targets from downstream regulatory changes. *Nucleic Acids*

856   *Research* **48**, 9724–9746.

857   Pearen M.A., Goode J.M., Fitzsimmons R.L., Eriksson N.A., Thomas G.P., Cowin G.J.

858   *et al.* (2013) Transgenic muscle-specific Nor-1 expression regulates multiple

859   pathways that effect adiposity, metabolism, and endurance. *Molecular*

860   *Endocrinology* **27**, 1897–1917.

861   Pérez-Montarelo D., Fernández A., Barragán C., Noguera J.L., Folch J.M., Rodríguez

862   M.C. *et al.* (2013) Transcriptional characterization of porcine leptin and leptin

863   receptor genes. *PLoS One* **8**, e66398.

864   Perttilä J., Merikanto K., Naukkarinen J., Surakka I., Martin N.W., Tanhuanpää K. *et al.*

865   (2009) *OSBPL10*, a novel candidate gene for high triglyceride trait in

866   dyslipidemic Finnish subjects, regulates cellular lipid metabolism. Journal of

867   Molecular Medicine **87**, 825–835.

868   Pilcher C.M., Jones C.K., Schroyen M., Severin A.J., Patience J.F., Tuggle C.K. *et al.*

869   (2015) Transcript profiles in longissimus dorsi muscle and subcutaneous adipose

870   tissue: A comparison of pigs with different postweaning growth rates. *Journal of*

871   *Animal Science* **93**, 2134–2143.

872   Pillman K.A., Scheer K.G., Hackett-Jones E., Saunders K., Bert A.G., Toubia J. *et al.*

873   (2019) Extensive transcriptional responses are co-ordinated by microRNAs as

874   revealed by Exon–Intron Split Analysis (EISA). *Nucleic Acids Research* **47**,

875   8606-8619.

876   Reverter A. & Chan E.K.F. (2008) Combining partial correlation and an information

877   theory approach to the reversed engineering of gene co-expression networks.

878   *Bioinformatics* **24**, 2491–2497.

879   Robinson M.D. & Oshlack A. (2010) A scaling normalization method for differential

880   expression analysis of RNA-seq data. *Genome Biology* **11**, R25.

881   Robinson M.D., McCarthy D.J. & Smyth G.K. (2010) edgeR: a Bioconductor package

882   for differential expression analysis of digital gene expression data.

883   *Bioinformatics* **26**, 139–40.

884   Schaefke B., Sun W., Li Y.-S., Feng L. & Chen W. (2018) The evolution of

885   posttranscriptional regulation. *Wiley Interdisciplinary Reviews* **9**, e1485.

886   Tamahara T., Ochiai K., Muto A., Kato Y., Sax N., Matsumoto M. *et al.* (2017) The

887   mTOR-Bach2 cascade controls cell cycle and class switch recombination during

888   B cell differentiation. Molecular and Cellular Biology **37**, e00418-17.

889   Tao R., Xiong X., Liangpunsakul S. & Dong X.C. (2015) Sestrin 3 protein enhances

890   hepatic insulin sensitivity by direct activation of the mTORC2-Akt signaling.

891   *Diabetes* **64**, 1211–1223.

892   Tarbier M., Mackowiak S.D., Frade J., Catuara-Solarz S., Biryukova I., Gelali E. *et al.*

893   (2020) Nuclear gene proximity and protein interactions shape transcript

894   covariations in mammalian single cells. *Nature Communications* **11**, 5445.

895   Ussar S., Bezy O., Blüher M. & Kahn C.R. (2012) Glypican-4 enhances insulin

896   signaling via interaction with the insulin receptor and serves as a novel

897   adipokine. *Diabetes* **61**, 2289–2298.

898   Wang Y., Yan S., Xiao B., Zuo S., Zhang Q., Chen G. *et al.* (2018) Prostaglandin F 2α

899   facilitates hepatic glucose production through CaMKIIγ/p38/FOXO1 signaling

900   pathway in fasting and obesity. *Diabetes* **67**, 1748–1760.

901   Warr A., Affara N., Aken B., Beiki H., Bickhart D.M., Billis K. *et al.* (2020) An

902   improved pig reference genome sequence to enable pig genetics and genomics

903   research. *Gigascience* **9**, 1–14.

904   Watson-Haigh N.S., Kadarmideen H.N. & Reverter A. (2010) PCIT: an R package for

905   weighted gene co-expression networks based on partial correlation and

906   information theory approaches. *Bioinformatics* **26**, 411–413.

907   Wu D., Hu D., Chen H., Shi G., Fetahu I.S., Wu F. *et al.* (2018) Glucose-regulated

908   phosphorylation of TET2 by AMPK reveals a pathway linking diabetes to cancer.

909   *Nature* **559**, 637–641.

910   Xie S., Li X., Qian L., Cai C., Xiao G., Jiang S. *et al.* (2019) An integrated analysis of

911   mRNA and miRNA in skeletal muscle from myostatin-edited Meishan pigs.

912   *Genome* **62**, 305–315.

913 Xu S., Ni H., Chen H. & Dai Q. (2019) The interaction between STAT3 and nAChRα1

914   interferes with nicotine-induced atherosclerosis via Akt/mTOR signaling

915   cascade. *Aging* **11**, 8120–8138.

916 Yang J. & Shi B. yin (2021) Dickkopf (Dkk)-2 is a beige fat-enriched adipokine to

917   regulate adipogenesis. *Biochemical and Biophysical Research Communications*

918   **548**, 211–216.

919 Zhang S., Hulver M.W., McMillan R.P., Cline M.A. & Gilbert E.R. (2014) The pivotal

920   role of pyruvate dehydrogenase kinases in metabolic flexibility. *Nutrition &*

921   *Metabolism* **11**, 10.

922

923

Supplementary Materials

925 **Figure S1:** Diagram depicting the routine/pipeline implemented for studying miRNA-

926 driven post-transcriptional regulatory signals applying the EISA approach and

927 additional enrichment and covariation analyses.

928 **Figure S2:** Diagram representing each one of the context-based filtering criteria used

929 for excluding *in silico*-predicted miRNA-mRNA interactions. AU: miRNA binding sites

930 with AU-rich flanking sequences (30 nts upstream and downstream). M: miRNA

931 binding sites located in the middle of the 3'-UTR sequence (45-55%). E: miRNA

932 binding sites located too close (< 15 nts) to the beginning or the end of the 3'-UTR

933 sequences.

934 **Figure S3:** Scatterplots depicting the exonic (ΔEx) and intronic (ΔInt) fractions of

935 expressed genes from *gluteus medius* skeletal muscle samples of fasting (*AL-T0*, N =

936 11) and fed (*AL-T2*, N = 12) Duroc gilts. (**a**) Genes differentially expressed and

937 showing either significant upregulation (FC > 2; *q*-value < 0.05, in green) or

938   downregulation (FC < -2, q-value < 0.05, in red) in fed (*AL-T2*, N = 12) Duroc gilts

939   with respect to their fasted (*AL-T0*, N = 11) counterparts. (**b**) Genes with the top 5%

940   post-transcriptional (PTc) negative scores and at least 2-fold reduced exonic (ΔEx)

941   fraction (equivalent to -1 in the $\log_2$ scale) are highlighted in purple.

942   **Figure S4:** Enrichment analyses comparing all expressed mRNA genes and the set of

943   mRNA genes with the (**a**) top 1% and (**b**) top 5% negative PTc scores and at least 2-fold

944   ΔEx reduction as being putatively targeted by significantly upregulated miRNAs (FC >

945   1.5; q-value < 0.05) from *gluteus medius* skeletal muscle samples of fasting (*AL-T0*, N =

946   11) and fed (*AL-T2*, N = 12) Duroc gilts. Results show the change in enrichment

947   significance (expressed as -$\log_{10}$ of the estimated *P*-value) when incorporating context-

948   based pruning of 8mer, 7mer-m8 and 7mer-A1 miRNA binding sites. R: Raw

949   enrichment analyses without any additional context-based pruning. AU: Enrichment

950   analyses removing miRNA binding sites without AU-rich flanking sequences (30 nts

951   upstream and downstream). M: Enrichment analyses removing miRNA binding sites

952   located in the middle of the 3'-UTR sequence (45-55%). E: Enrichment analyses

953   removing miRNA binding sites located too close (< 15 nts) to the beginning or the end

954   of the 3'-UTR sequences. The dashed line represents a nominal *P*-value of 0.05 set as

955   significance threshold.

956   **Figure S5:** Quantification of selected genes and miRNAs expressed in the pig adipose

957   tissue by qPCR. (**a**) Barplots depicting qPCR $\log_2$ transformed relative quantities (Rq)

958   for *LEP, OSBPL10, PRSS23, RNF157* and *SERPINE2* mRNA transcripts measured in

959   adipocytes from the retroperitoneal fat of *lean* (N = 5) and *obese* (N = 5) UNIK

960   minipigs. (**b**) Barplots depicting qPCR $\log_2$ transformed relative quantities (Rq) for ssc-

961   miR-148a-3p, ssc-miR-214-3p and ssc-miR-92b-3p miRNA transcripts measured in

962   isolated adipocytes from the retroperitoneal fat of *lean* (N = 5) and *obese* (N = 5) UNIK

963   minipigs. All the analyzed mRNA genes showed a reduced expression in *lean* minipigs

964   compared with their *obese* counterparts, and the *LEP* gene was the most significantly

965   downregulated gene. For miRNAs, the opposite pattern of expression was observed,

966   being all of them upregulated in *lean* minipigs. Moreover, ssc-miR-92b-3p showed the

967   most significant increased expression in *lean* minipigs, in agreement with results

968   obtained in differential expression analyses (**Table S10**).

969

970   **Table S1:** Phenotypic values of body mass index (BMI) trait and sex classification

971   recorded in 11 Duroc-Göttingen minipigs from the F2-UNIK resource population and

972   grouped as *obese* or *lean* in accordance with their BMI.

973   **Table S2:** Primers for qPCR verification of selected mRNAs and miRNAs in the F2-

974   UNIK Duroc-Göttingen minipig population after comparing *lean* (N = 5) and *obese* (N

975   = 5) individuals.

976   **Table S3:** Raw Cq values obtained in qPCR analyses measuring adipocyte expression

977   levels of selected mRNAs and miRNAs from *lean* (N = 5) and *obese* (N = 5) UNIK

978   minipigs.

979   **Table S4:** Differential expression analyses of RNA-seq data using the *edgeR* tool and

980   comparing *gluteus medius* expression profiles of fasted *AL-T0* (N = 11) and fed *AL-T2*

981   (N = 12) Duroc gilts. (**a**) Differentially expressed genes (q-value < 0.05, N = 454). In

982   bold are genes either upregulated (N = 52) or downregulated (N = 80) with |FC| > 2 and

983   q-value < 0.05. (**b**) Differential expression results for genes with top 5% post-

984   transcriptional (PTc) scores and at least 2-fold reduced exonic fraction (ΔEx)

985   (equivalent to -1 in the $\log_2$ scale). The 18 genes with FC < -2 and *q*-value < 0.05 are

986   shown in bold. (**c**) Differential expression results showing the whole list of expressed

987   genes with an average expression above 1 CPM in at least 50% of samples within each

988   group (N = 9,492).

989   **Table S5:** Differential expression analyses of microRNAs using the *edgeR* tool and

990   comparing *gluteus medius* expression levels of fasted *AL-T0* (N = 11) and fed *AL-T2* (N

991   = 12) Duroc gilts. In bold are microRNAs detected as significantly differentially

992   expressed (|FC| > 1.5; *q*-value < 0.05, N = 16).

993   **Table S6:** Post-transcriptional (PTc) and transcriptional (Tc) signals detected with

994   EISA in genes expressed in *gluteus medius* skeletal muscle samples from fasted (*AL-T0*,

995   N = 11) and fed (*AL-T2*, N = 12) Duroc gilts. (**a**) Genes with significant PTc scores

996   (|FC| > 2; *q*-value < 0.05, N = 133). In bold are genes with at least 2-fold reduced ΔEx

997   fraction (N = 3). (**b**) Genes with significant Tc scores (|FC| > 2; *q*-value < 0.05, N =

998   344). In bold are genes also significant in their PTc scores (|FC| > 2; *q*-value < 0.05, N =

999   91). EISA results showing the whole list of genes with an average expression above 1

1000   CPM in at least 50% of samples within each group (N = 9,492) and their (**c**) PTc and (**d**)

1001   Tc scores.

1002   **Table S7:** Binding sites in the 3'-UTRs of mRNA genes (with the top 5% negative PTc

1003   scores and at least 2-fold reduction in the exonic fraction) predicted as targets (N = 21)

1004   of non-redundant significantly upregulated miRNAs (N = 6) expressed in the *gluteus*

1005   *medius* skeletal muscle samples from fasting (*AL-T0*, N = 11) and fed (*AL-T2*, N = 12)

1006   Duroc gilts.

1007   **Table S8:** Covariation enrichment scores (CES) for the exonic and intronic fractions of

1008   mRNA genes (with the top 5% negative post-transcriptional signals PTc and at least 2-

1009   fold reduction in their exonic ΔEx fraction) predicted as targets of non-redundant

1010   significantly upregulated miRNAs (N = 6) expressed in *gluteus medius* skeletal muscle

1011   samples from fasting (*AL-T0*, N = 11) and fed (*AL-T2*, N = 12) Duroc gilts.

43

1012   **Table S9:** Differential expression analyses of RNA-seq data using the *edgeR* tool and

1013   comparing adipocyte expression profiles of *lean* (N = 5) and *obese* (N = 5) UNIK

1014   minipigs classified in accordance with their body mass index. (**a**) Differentially

1015   expressed genes (*q*-value < 0.05, N = 299). In bold are genes either upregulated (N =

1016   52) or downregulated (N = 95) with |FC| > 2 and *q*-value < 0.05. (**b**) Differential

1017   expression results for genes with top 5% post-transcriptional (PTc) scores and at least 2-

1018   fold reduced exonic fraction (ΔEx) (equivalent to -1 in the $\log_2$ scale). The 12 genes

1019   with FC < -2 and *q*-value < 0.05 are shown in bold. (**c**) Differential expression results

1020   showing the whole list of expressed genes with an average expression above 1 CPM in

1021   at least 50% of samples within each group (N = 9,746).

1022   **Table S10:** Differential expression analyses of microRNAs using the *edgeR* tool and

1023   comparing adipocyte expression profiles from *lean* (N = 5) and *obese* (N = 5) UNIK

1024   minipigs classified in accordance with their body mass index. In bold are microRNAs

1025   detected as significantly differentially expressed (|FC| > 1.5; *P*-value < 0.01, N = 7).

1026   **Table S11:** Post-transcriptional (PTc) and transcriptional (Tc) signals detected with

1027   EISA in genes expressed in adipocytes from *lean* (N = 5) and *obese* (N = 5) UNIK

1028   minipigs classified in accordance with their body mass index. (**a**) Genes with significant

1029   PTc scores (|FC| > 2; *q*-value < 0.05, N = 1). In bold are genes with at least 2-fold

1030   reduced ΔEx fractions (N = 1). (**b**) Genes with significant Tc scores (|FC| > 2; *q*-value <

1031   0.05, N = 195). In bold are genes also among the top 5% negative PTc scores and at

1032   least 2-fold ΔEx reduction (N = 3). EISA results showing the whole list of genes with

1033   an average expression above 1 CPM in at least 50% of samples within each group (N =

1034   9,746) and their (**c**) PTc and (**d**) Tc scores.

1035   **Table S12:** Binding sites in the 3'-UTRs of mRNA genes (with the top 5% negative

1036   PTc scores and at least 2-fold reduction in the exonic fraction) predicted as targets (N =

1037   25) of non-redundant significantly upregulated miRNAs (N = 4) expressed in

1038   adipocytes from *lean* (N = 5) and *obese* (N = 5) UNIK minipigs.

1039   **Table S13:** Covariation enrichment scores (CES) for the exonic and intronic fractions

1040   of mRNA genes (with the top 5% negative post-transcriptional signals PTc and at least

1041   2-fold reduction in their exonic ΔEx fraction) predicted as targets of non-redundant

1042   significantly upregulated miRNAs (N = 4) expressed in adipocytes from *lean* (N = 5)

1043   and *obese* (N = 5) UNIK minipigs.